Journal of Tropical Biodiversity and Biotechnology
Volume 11, Issue 02 (2026): jtbb20876
DOI: 10.22146/jtbb.20876

Research Article

Thermophilic Biosurfactant-Mediated Stabilization of Silver Nanoparticles by *Aeribacillus pallidus*

Mark Joseph R. Remucal[1,2*], Francis Ruel G. Castillo[1,3], May Enaccel S. Macalan[1,4], Ronan Q. Baculi[1,5]

1)Department of Biology, College of Science, University of the Philippines Baguio, Baguio City, 2600, Philippines
2)Biological Models Laboratory, Department of Biochemistry and Molecular Biology, College of Medicine, University of the Philippines Manila, Taft Avenue, Ermita, Manila, 1000, Philippines
3)College of Medicine, University of the Philippines Manila, Taft Avenue, Ermita, Manila, 1000, Philippines
4)Philippine General Hospital, University of the Philippines Manila, Taft Avenue, Ermita, Manila, 1000, Philippines
5)Microbial Oceanography Laboratory, Marine Science Institute, University of the Philippines Diliman, Quezon City 1101 Philippines
* Corresponding author, email: mrremucal@up.edu.ph

Keywords:
Aeribacillus pallidus
Biosurfactant
Green synthesis
Silver nanoparticles
Thermophiles
Submitted:
18 April 2025
Accepted:
26 August 2025
Published:
03 April 2026
Editors:
Miftahul Ilmi
Liya Audinah

ABSTRACT

The biosynthesis of silver nanoparticles (AgNPs) using microorganisms is an eco-friendly approach that reduces the environmental impact of conventional chemical methods. This study focuses on the utilization of the thermophilic bacterium *Aeribacillus pallidus*, isolated from the Badekbek hot spring in Bokod, Benguet, Philippines, to synthesize AgNPs through biosurfactant-mediated reduction of $AgNO_3$ in a reverse micelle system. Scanning electron microscopy (SEM) analysis revealed that biosurfactant-stabilized AgNPs exhibited spherical to amorphous shapes with a uniform size distribution ranging from 1.12 nm to 32.45 nm and an average size of 9.65 ± 5.74 nm. In contrast, nonstabilized AgNPs displayed irregular morphologies due to significant agglomeration, with sizes from 4.92 nm to 162.99 nm and an average of 29.20 ± 21.52 nm. Fourier-transform infrared (FTIR) spectroscopy indicated the presence of functional groups in the biosurfactant that likely contributed to the stabilization of AgNPs, reducing their tendency to aggregate. Energy dispersive X-ray (EDX) analysis confirmed the high silver content in both biosurfactant-stabilized (83.43 %) and nonstabilized (84.61 %) AgNPs, with a notable increase in oxygen (6.59 %) and carbon (9.31 %) concentrations in the biosurfactant-stabilized nanoparticles, correlating with the FTIR results. The findings suggest that the biosurfactants produced by *A. pallidus* effectively mitigate nanoparticle aggregation, enhancing the stability and quality of the synthesized AgNPs. This proof-of-concept study highlights the potential of thermophilic biosurfactants for green synthesis, while recognizing that validation of their biological and industrial applications requires further investigation.

How to cite:
Remucal, M.J.R. et al., 2026. Thermophilic Biosurfactant-Mediated Stabilization of Silver Nanoparticles by *Aeribacillus pallidus*. *Journal of Tropical Biodiversity and Biotechnology*, 11(2), jtbb20876. doi: 10.22146/jtbb.20876

INTRODUCTION

The biosynthesis of nanoparticles, also known as green synthesis, is an emerging approach that aims to reduce the environmental impact associated with conventional chemical methods. This eco-friendly process leverages the ability of biological entities, such as microorganisms, plants, and enzymes, to reduce metal ions and produce nanoparticles (Osman et al. 2024). The use of microorganisms, in particular, has gained attention due to their ability to produce nanoparticles with well-controlled morphology and properties (Albukhaty et al. 2025). Microbial biosynthesis can occur either intracellularly, where whole cells reduce metal ions through enzymatic activity, or extracellularly, where cell-free supernatants containing enzymes, proteins, reducing sugars, and biosurfactants mediate both reduction and stabilization (Vanlalveni et al. 2024). Silver nanoparticles (AgNPs) synthesized through microbial processes have been reported to exhibit numerous advantageous characteristics, such as high stability, uniform particle size distribution, and biocompatibility (Osman et al. 2024; Saleem et al. 2023).

One major challenge in nanoparticle synthesis is controlling the aggregation of particles, as aggregation can lead to inconsistent particle sizes and reduced functionality (Shrestha et al. 2020). To address this issue, biosurfactants produced by microorganisms are increasingly being utilized for stabilizing nanoparticles (Saleem et al. 2023). Biosurfactants are amphiphilic compounds that reduce surface tension and provide a protective layer around nanoparticles, thereby preventing aggregation and enhancing their stability. Biosurfactant-producing bacteria have been identified as effective agents for nanoparticle stabilization (Busscher et al. 1994; Kim et al. 1997; Zheng et al. 2012). The use of biosurfactants in nanoparticle synthesis not only promotes a greener and more sustainable approach but also improves the uniformity and stability of nanoparticles (Singla et al. 2017). Biosurfactants can act both as natural bioreductants that convert metal ions into nanoparticles and as capping agents that prevent aggregation, making them important mediators of environmentally friendly AgNP synthesis (Zehra et al. 2025).

Thermophilic bacteria, which can thrive in high-temperature environments (50 °C or higher), have also demonstrated potential in nanoparticle synthesis. Examples include *Ureibacillus thermosphaericus*, which has been used to synthesize both gold and silver nanoparticles (Juibari et al. 2011), and *Geobacillus stearothermophilus* for the synthesis of gold and silver nanoparticles (Fayez et al. 2011). Thermophiles are particularly advantageous due to their ability to withstand harsh conditions, making them ideal for nanoparticle synthesis in environments with fluctuating temperatures and pH. Biosurfactant-producing bacteria that can be isolated from extreme environments, such as thermophiles, are particularly significant in the biosynthesis of nanoparticles. These bacteria are adapted to thrive in harsh conditions, such as high temperatures, which often make traditional synthesis challenging. Their ability to produce biosurfactants under such conditions is especially beneficial for stabilizing nanoparticles, as the biosurfactants help maintain the uniformity and dispersion of nanoparticles (Juibari et al. 2011). Thermophiles are thus valuable not only for their resilience but also for their contribution to green nanoparticle synthesis by generating biosurfactants that prevent aggregation and provide enhanced stability (Fayez et al. 2011).

Thermophilic biosurfactants exhibit inherent stability at elevated temperatures, which enhances their effectiveness in applications that require high thermal resistance. This thermal stability provides thermophilic biosurfactants with an advantage over those produced by mesophilic bacteria that thrive at temperatures between 20 to 45 °C, which may lose their efficiency at higher temperatures, limiting their applicability in such scenarios (Mehetre et al. 2019; Sarubbo et al. 2022). Furthermore, biosurfactants produced by thermophilic bacteria are highly effective in emulsification and surface tension reduction, even in harsh environments, which makes them particularly useful for industrial processes like oil degradation at elevated temperatures—a benefit not typically observed with biosurfactants from mesophilic bacteria (Sarubbo et al. 2022; Schultz et al. 2022).

Biosurfactant-stabilized nanoparticles have been observed to show promising stability, allowing them to be stored for extended periods (Płaza et al. 2014). The stabilization provided by biosurfactants leads to improved nanoparticle quality with a uniform size distribution, which is crucial for practical applications in various fields, including medicine, agriculture, and environmental remediation. By utilizing biosurfactants, the synthesis process becomes more efficient and environmentally friendly, eliminating the need for harsh chemical stabilizing agents (Markam et al. 2024).

In this study, we aimed to isolate a thermophilic biosurfactant-producing bacterium and evaluate its ability to mediate the green synthesis of silver nanoparticles. The synthesized nanoparticles were characterized using UV–Vis spectroscopy, SEM, FTIR, and EDX analyses to assess their morphology, stability, and elemental composition.

MATERIALS AND METHODS

Sample collection and isolation of thermophilic bacteria

Water samples were collected at different points from the Badekbek hot spring in Bokod, Benguet, Philippines using sterile thermal flasks. Collected water samples were immediately inoculated onto Thermus media by adding 10 mL of the water sample to 90 mL of Thermus media with the following composition (in grams per liter of deionized water): $CaSO_4{\cdot}2H_2O$ (0.06), $MgSO_4{\cdot}7H_2O$ (0,1), NaCl (1), KNO_3 (0.103), NaNO3 (0.689), Na_2HPO_4 (0.111), $FeCl_3$ (0.02), $MnSO_4{\cdot}H_2O$ (0.022), $ZnSO_4{\cdot}7H_2O$ (0.05), H_3BO_3 (0.05), $CuSO_4$ (0.002), $Na_2MoO_4{\cdot}2H_2O$ (0.003), $CoCl_2{\cdot}2H_2O$ (0.05), EDTA (0.06), yeast extract (1), and peptone (0.5) (Brock & Freeze 1969). Concentrated H_2SO_4 was added to adjust the pH to 7.0. The Thermus broth solutions were incubated at 60 °C for 72 h. Samples from the Thermus broth solutions were serially diluted and subsequently plated onto respective solidified medium plates using agar (2 %) as a solidifying agent. Before plating, $MgSO_4$ (0.5 %) was also added to make the agar solidifying agent heat stable (Brock & Freeze 1969). All plates were incubated for 72 h at 60 °C. Morphologically distinct colonies on the plates were selected and subjected to repeated streak plating on a solidified Thermus medium. Pure isolates were suspended in Thermus broth containing 20 % glycerol and stored at -20 °C until use.

Screening, Extraction, and Characterization of Biosurfactant-Producing Thermophilic Bacteria

To screen for biosurfactant-producing thermophilic bacteria, 50 mL of mineral salt medium (MSM) (Arutchelvi et al. 2009) was dispensed into 250 mL Erlenmeyer flasks. The MSM contained (in grams per liter of deionized water): K_2HPO_4 (1.0), KH_2PO_4 (0.5), NH_4NO_3 (4.0), KCl (0.1), $MgSO_4{\cdot}7H_2O$ (0.5), $FeSO_4{\cdot}7H_2O$ (0.01), $CaCl_2$ (0.01), yeast extract (0.1), and a trace element solution (10 mL) consisting of $ZnSO_4{\cdot}7H_2O$ (0.7), $MnSO_4{\cdot}7H_2O$ (0.5), $CuSO_4{\cdot}5H_2O$ (0.5), H_3BO_3 (0.26), and $(NH_4)_6Mo_7O_2{\cdot}4H_2O$ (0.06) (Yateem et al. 2002). The pH was adjusted to 7.0. To this medium, 1 mL of crude oil and glucose were added to serve as carbon and energy sources. The flasks were inoculated with 1 mL bacterial culture and incubated at 55 °C under shaking conditions (180 rpm) for 7 days. After incubation, the medium was centrifuged at 4 °C, 10,000 rpm for 15 minutes to obtain a cell-free liquid, which was mixed with acetone (1:1,v v^{-1}) and left at 4 °C for 24 h. The precipitate was subjected to centrifugation at 4000 rpm for 15 minutes at 5 °C to obtain the crude extract, which was then resuspended in deionized water.

The extracted biosurfactant was characterized using Fourier Transform Infrared Spectroscopy (FTIR; Nicolet iS10, Thermo Fisher Scientific, USA) to identify functional groups and bond types within a range of 4000 to 500 cm $^{-1}$. The crude biosurfactant was air dried for 48 h before analysis, based on the extraction method described by Jara et al. (2013).

Identification of biosurfactant-producing thermophilic bacteria

Pure cultures of bacterial isolates capable of producing biosurfactants were sent to Macrogen, Inc. in South Korea for amplification and sequencing of the 16S rRNA genes. Amplification and sequencing of the 16S rRNA gene was carried out using universal bacterial primers 27F (AGAGTTTGATCCTGGCTCAG) and 1492R (GGGTTACCTTGTTACGACTT), and another sequencing was performed with internal primers 785F (GGATTAGATACCCTGGTA) and 907R (CCGTCAATTCMTTTRAGTTT) to obtain high-quality overlapping reads covering the full gene length for more accurate species identification. The sequences were manually evaluated using Chromas Pro Software to eliminate low-quality regions typically found at the beginning and end of the fragments. The DNA sequences were analyzed using the BLAST tool available at the National Center for Biotechnology Information (NCBI) server (http://blast.ncbi.nlm.nih.gov) and compared against the nucleotide sequence BLAST tool.

Biosurfactant-mediated Synthesis of AgNPs

The synthesis of AgNPs using biosurfactant was adapted from Farias et al. (2014), with modifications as described below. Briefly, 1 mL of 0.1 g L^{-1} of biosurfactant was dissolved in a mixture of 1 mL of 0.05 M aqueous $AgNO_3$ and 6.25 mL of n-heptane. The solution was stirred vigorously at room temperature for 10 minutes or until homogenization is achieved. Then, 1 mL of 0.1 M aqueous $NaBH_4$ solution was added to the mixture and was stirred vigorously for 30 minutes. To break the reverse micelles, 10 mL of ethanol was added to the mixture and the precipitate was separated by repeated centrifugation at 10,000 rpm for 30 minutes at room temperature. The collected precipitate was washed with 1 mL sterile distilled water and 10 mL of n-butanol was added to form a suspension with the aid of sonication. The precipitate was subsequently air-dried at room temperature in the laminar hood. Control set-up without biosurfactant was also carried out under identical conditions.

Characterization of Biosurfactant-Stabilized AgNPs

The synthesized biosurfactant-stabilized AgNPs was characterized by UV-Vis spectrophotometry (UV-1800, Shimadzu, Japan) at wavelengths 300 to 800 nm range and was monitored every 8 h within 24 h incubation time. Qualitative and quantitative analyses were performed using scanning electron microscopy (SEM; JSM-7610F, JEOL Ltd., Japan), and energy dispersive X-Ray spectroscopy (EDX; Oxford X-MaxN, Oxford Instruments, UK) to determine the size, shape, and elemental composition of the biosurfactant-stabilized AgNPs. The average particle size distributions of the AgNPs were determined by calculating the mean of 500 particles from the micrographs, utilizing IMAGE J 1.46r software. Infrared spectra of the sample were recorded using Fourier Transform Infrared (FTIR) spectroscopy in the 4000-600 cm^{-1} necessary for the detection of various functional groups of the biosurfactant involved in stabilization of the AgNPs.

RESULTS AND DISCUSSION

Identification of biosurfactant-producing bacteria

Twelve morphologically distinct bacterial isolates were obtained and screened for biosurfactant production. The initial screening was performed using oil displacement test and emulsification index (E24) assay adapted from Nayarisseri et al. (2018). The isolate producing the highest amount of biosurfactant after 7 days of incubation was selected for further analysis. BLAST analysis of the near full-length 16S rRNA gene sequence indicated 100 % query coverage and 99.99 % identity to *A. pallidus* strain EF60115 (GenBank accession MW132409.1). The isolate grew optimally at 55 °C and was able to grow within a temperature range of 50–60 °C, confirming its thermophilic nature (Lee et al. 2022).

Characterization of biosurfactant

The FTIR spectra of the biosurfactant produced by *A. pallidus* revealed a heteropolymeric nature, as evidenced by the diverse functional groups detected (Figure 1). The broad band at 3405 cm^{-1} corresponds to O–H stretching, indicating the presence of hydroxyl groups, while the band at 2925 cm^{-1} is associated with C–H stretching, characteristic of aliphatic chains. These results align with findings by Zheng et al. (2012), who reported similar broad peaks around 3428 cm^{-1} and 2923 cm^{-1} in biosurfactants produced by *A. pallidus*, indicating hydroxyl and alkane groups, respectively.

The FTIR spectrum also displayed a band at 1623 cm^{-1}, consistent with an amide group, suggesting the presence of protein or peptide components. A peak at 1384 cm^{-1} suggests the presence of carboxyl groups, while a peak at 1105 cm^{-1} is indicative of ester groups. The absorption peaks at 668 cm^{-1} and 602 cm^{-1} suggest the presence of phosphate groups in the biosurfactant (Gonzaga et al. 2005).

Overall, the FTIR analysis indicated that the biosurfactant produced by *A. pallidus* contains functional groups such as hydroxyl, alkane, amide, carboxyl, ester, and phosphate, highlighting its complex heteropolymeric composition. This diverse range of functional groups suggests the biosurfactant may have versatile surface-active properties suitable for various applications.

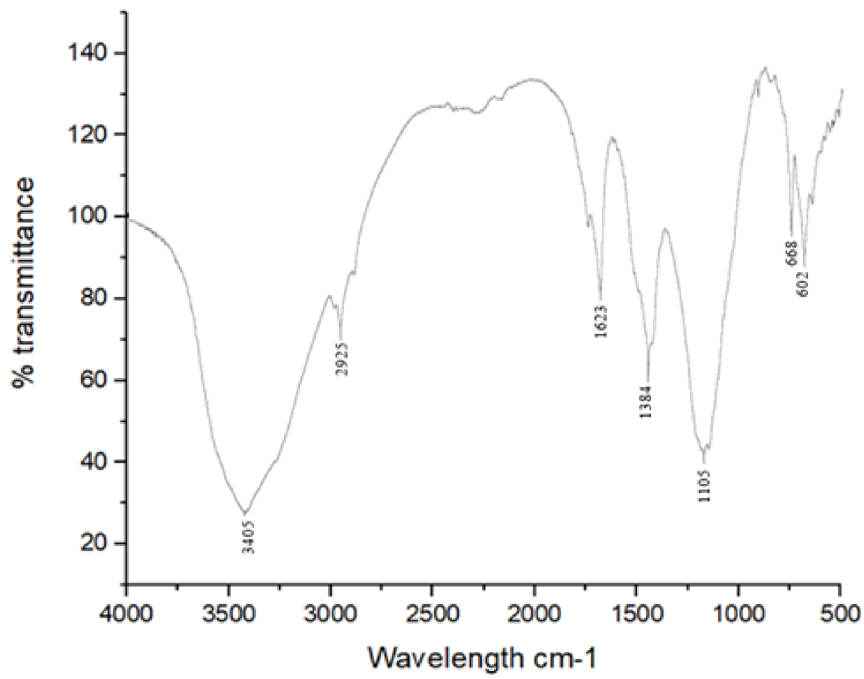

Figure 1. FTIR spectra of biosurfactant extracted from *A. pallidus* showing the presence of carboxyl (1384 cm^{-1}), ester (1105 cm^{-1}), hydroxyl (3405 cm^{-1}), alkane (2925 cm^{-1}), amide (1623 cm^{-1}), and phosphate (668 cm^{-1} and 602 cm^{-1}) groups.

Biosynthesis and UV-Vis characterization of stabilized and nonstabilized silver AgNPs

AgNPs were synthesized both with and without a biosurfactant. For the stabilized AgNPs, biosurfactant was added to the reaction mixture containing $AgNO_3$, $NaBH_4$, and n-hexane at 37 °C and pH 7, whereas for the nonstabilized AgNPs, biosurfactant was omitted under identical conditions. UV-Vis spectrophotometric analysis was performed after 24 h of incubation to measure the surface plasmon resonance (SPR) peaks, which are indicative of nanoparticle formation.

The stabilized AgNPs showed a characteristic UV-Vis absorption band at 430 nm (Figure 2), consistent with the typical SPR range for silver nanoparticles (420–430 nm) (Yong et al. 2002). The nonstabilized AgNPs also exhibited an absorption peak at 430 nm, along with a minor absorption band at 500 nm, likely indicating polydispersity in nanoparticle size or shape. The aggregation of nanoparticles, as described by Yeh et al. (2011), could lead to the broadening of the SPR band, as nanoparticles in close proximity tend to agglomerate. This sensitivity of plasmonic nanoparticles results in collective oscillation of surface electrons, contributing to the observed spectral features.

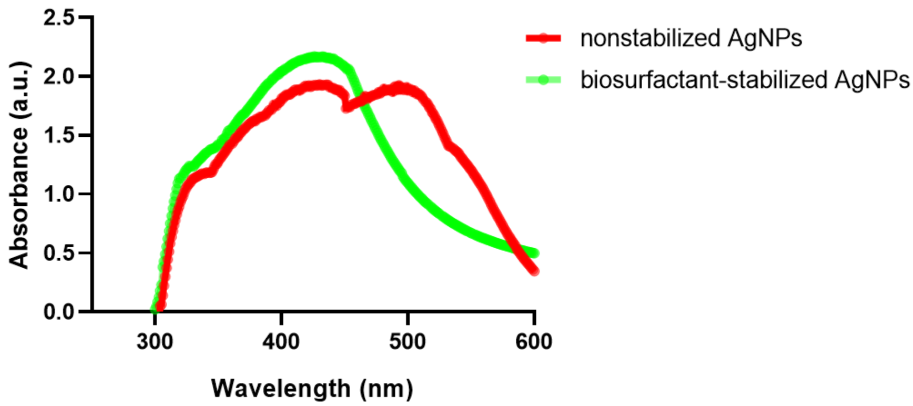

Figure 2. UV-Vis absorption spectra indicating the synthesis of biosurfactant-stabilized and nonstabilized AgNPs using biosurfactant extracted from *A. pallidus* (A) and nonstabilized AgNPs (B) after 24h incubation period.

The results of the UV-Vis characterization of AgNPs suggest that the biosurfactant plays a crucial role in stabilizing and controlling nanoparticle formation. It has been hypothesized that the aliphatic groups in the biosurfactant could form reverse micelles, acting as microreactors (Płaza et al. 2014). In such a microreactor-mediated borohydride reduction process, interactions between reverse micelles lead to collisions, facilitating the exchange of molecules within the micelles and promoting the formation of monomeric silver nuclei. These silver nuclei then grow within the micelles in a size-controlled manner (Płaza et al. 2014).

The role of biosurfactant in influencing the particle size distribution and monodispersity of silver nanoparticles is well-established. Specifically, the molar ratio of water to biosurfactant has been shown to be critical in controlling nanoparticle morphology and size (Płaza et al. 2014). In the current study, the water-to-biosurfactant ratio was kept constant, potentially explaining the observed uniformity in the surface plasmon resonance (SPR) band at 430 nm for the stabilized AgNPs. The minor aborptio band observed at 500 nm for nonstabilized AgNPs suggests polydispersity, which might be attributed to the lack of a stabilizing biosurfactant, leading to nanoparticle aggregation.

This aggregation phenomenon, as explained by Yeh et al. (2011), occurs due to the broadening of the SPR band, as nanoparticles in close proximity tend to agglomerate. The sensitivity of these plasmonic nanoparticles results in collective oscillation of surface electrons, contributing to changes in the observed absorption spectra. Therefore, the use of a biosurfactant not only aids in nanoparticle stabilization but also contributes to achieving a more uniform size distribution, minimizing agglomeration and enhancing the overall quality of the synthesized nanoparticles.

Scanning electron microscopy (SEM) analysis of biosurfactant-stabilized AgNPs

SEM analysis provided significant insights into the morphology and size distribution of biosurfactant-stabilized AgNPs. Nonstabilized AgNPs displayed irregular morphologies characterized by notable agglomeration, with sizes varying from 4.92 nm to 162.99 nm and an average size of 29.20 ± 21.52 nm (Figure 3C). In contrast, biosurfactant-stabilized AgNPs predominantly exhibited spherical to amorphous shapes, with a relatively uniform size distribution ranging from 1.12 nm to 32.45 nm and an average size of 9.65 ± 5.74 nm (Figure 3D). Notably, the majority of biosurfactant-stabilized nanoparticles were concentrated in the 1-8 nm range, while the nonstabilized nanoparticles were predominantly found within the 8-15 nm range (Figure 3). An independent samples t-test revealed a statistically significant difference in average sizes between the biosurfactant-stabilized AgNPs and non-stabilized AgNPs ($p < 0.01$), indicating that the stabilization process significantly influenced their size distribution and morphology.

The significant differences in size and morphology between biosurfactant-stabilized and nonstabilized AgNPs underscore the protective role of biosurfactant molecules from *A. pallidus*. The presence of these molecules not only prevents particle aggregation but also reduces the probability of nanoparticle collision and coalescence, attributed to the interaction between the biosurfactant's functional groups and the nanoparticles. This stabilization mechanism aligns with previous findings from Xie et al. (2006), who reported the synthesis of spherical nanoparticles sized 2-8 nm stabilized by the biosurfactant rhamnolipid in heptane, indicating that surfactant molecules effectively inhibit nanoparticle adherence. Moreover, Reddy et al. (2009) emphasized the role of free hydroxyl groups in biosurfactants, which create steric hindrance around nanoparticles through electrostatic interactions, further supporting the observed reduction in agglomeration. The formation of spherical AgNPs can be attributed to the micellar structure formed by the biosurfactant, which favors spherical nanoparticle formation during synthesis, as noted by Farias et al. (2014). Conversely, the lack of biosurfactant in the synthesis process resulted in the coalescence of AgNPs into larger aggregates, referred to as secondary nanoparticles (Singh et al. 2017).

In the absence of biosurfactant, $NaBH_4$ was still able to reduce Ag^+ to Ag^0; however, without micellar confinement or capping, the reduced silver rapidly aggregated, producing unstable particles with no persistent colloidal dispersion (Sidhu et al. 2022; Hardini & Saraswati 2023). This explains the absence of a defined SPR band observed in the nonstabilized sample, underscoring the role of biosurfactants in nanoparticle stabilization.

Energy dispersive x-ray (EDX) analysis of biosurfactant-stabilized and nonstabilized AgNPs

The EDX analysis revealed strong peaks corresponding to elemental silver in both biosurfactant-stabilized and nonstabilized AgNPs, indicating silver compositions of 83.43 % and 84.61 %, respectively (Figure 4). These findings confirm the successful synthesis of silver nanoparticles, as evidenced by the characteristic optical absorption peak at 3 keV, which is attributed to the surface

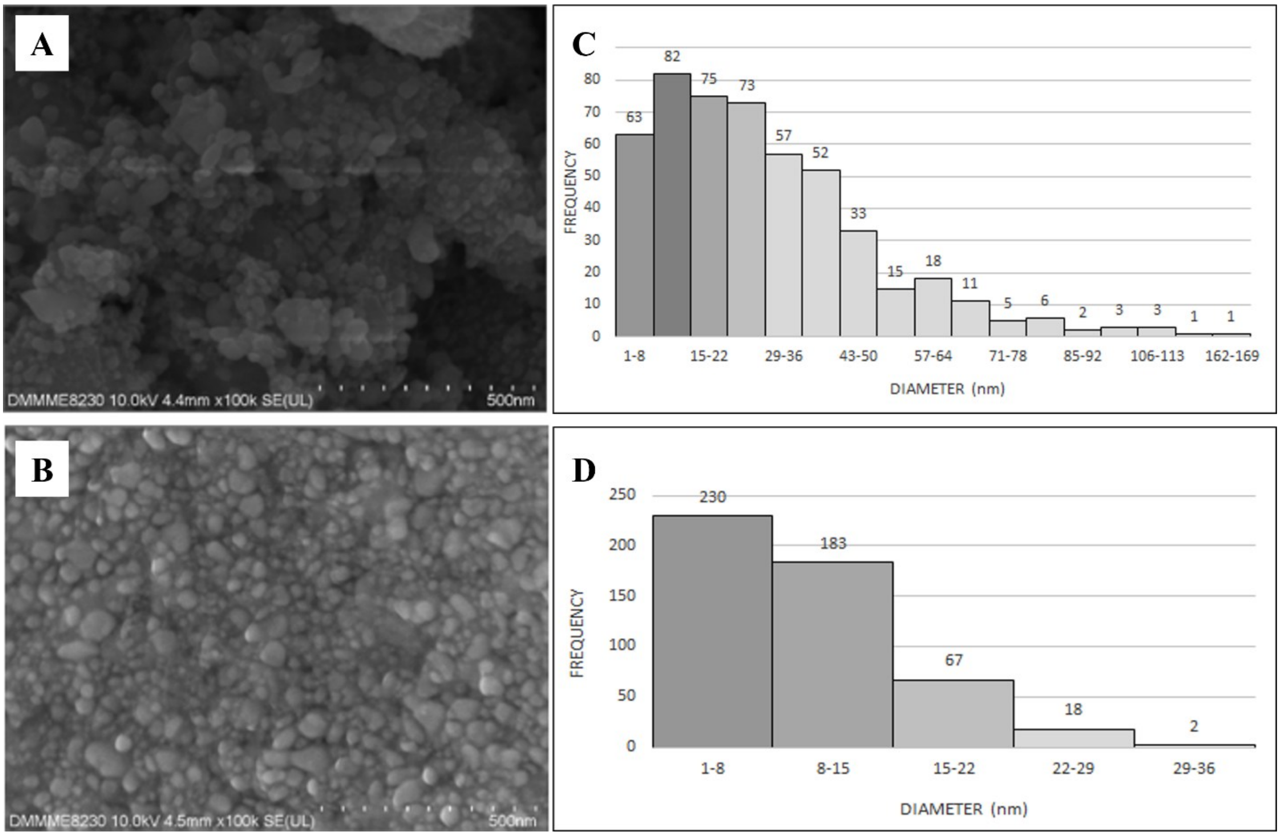

Figure 3. SEM images showing the size and morphology of the nonstabilized AgNPs (A) and biosurfactant-stabilized AgNPs (B); and Particle size distribution graph of nonstabilized (C) and biosurfactant-stabilized (D) AgNPs with a sample size of five hundred nanoparticles.

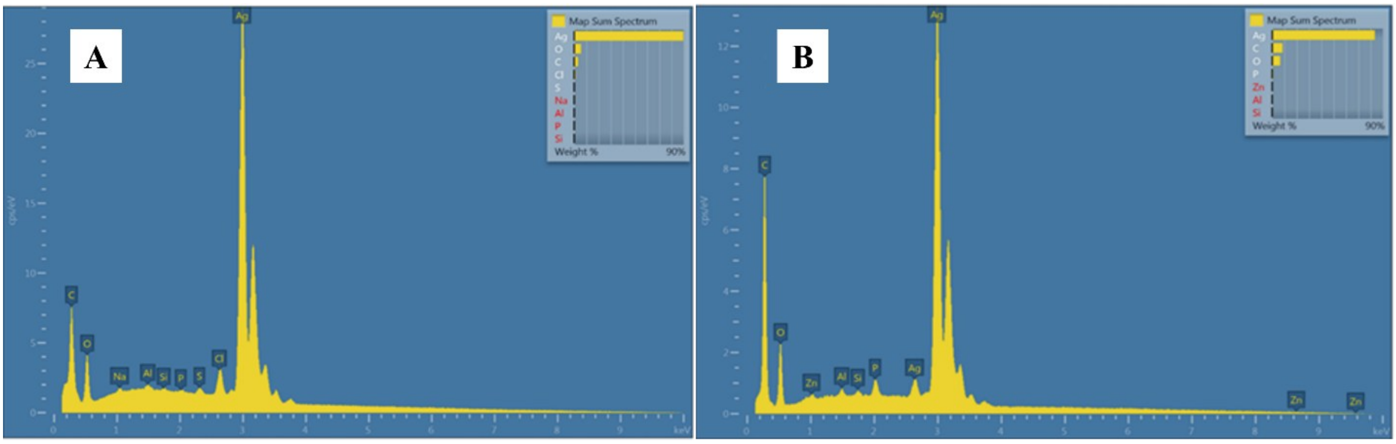

Figure 4. EDX spectra of nonstabilized (A) and biosurfactant-stabilized AgNPs (B) showing strong peak for Ag^{+}.

plasmon resonance of metallic silver nanoparticles (Hebeish et al. 2013; Gomaa 2016).

Interestingly, the oxygen concentration in biosurfactant-stabilized AgNPs was measured at 6.59 %, higher than the 5.03 % observed in nonstabilized AgNPs. similarly, the carbon content was also higher in biosurfactant-stabilized AgNPs, with 9.31 % compared to 7.06 % in nonstabilized AgNPs. This difference aligns with the FTIR analysis results, which indicated the presence of hydroxyl groups in the biosurfactant produced by *A. pallidus*. The hydroxyl groups play a crucial role in stabilizing the synthesized nanoparticles, as highlighted by Reddy et al. (2009) and Tomah et al. (2020). Furthermore, the higher trace peaks for carbon (C) and oxygen (O) in the EDX profile of biosurfactant-stabilized AgNPs suggests that functional groups such as carboxyl, ester, and alkane groups, derived from the biosurfactant, contribute to the stabilization of the nanoparticles.

Fourier-transform infrared spectroscopy (FTIR) analysis of AgNPs

The FTIR analysis was conducted to identify the functional groups in the biosurfactant that are potentially responsible for the stabilization of AgNPs (Figure 5). The FTIR spectrum of the biosurfactant-stabilized AgNPs exhibited peaks at 3591 cm^{-1}, 3572 cm^{-1}, and 3330 cm^{-1}, which correspond to hydroxyl groups (Tomah et al. 2020). This is consistent with the FTIR results for the biosurfactant (Figure 3), where a broad peak at 3405 cm^{-1} also indicated hydroxyl groups, suggesting their involvement in the stabilization of AgNPs (Kumar & Mamidyala 2011).

The absorption peaks at 2958 cm^{-1} and 2873 cm^{-1} are attributed to C–H stretching of alkane groups, similar to the band observed at 2925 cm^{-1} in the biosurfactant spectrum, which indicates the presence of aliphatic chains. Additionally, a peak at 1462 cm^{-1} also indicated C–H stretching of alkane groups, reinforcing the presence of hydrophobic components contributing to nanoparticle stabilization. The peaks between 1658 and 1631 cm^{-1} correspond to C=O stretching, which is characteristic of amide groups. This observation is in agreement with the amide band detected at 1623 cm^{-1} in the biosurfactant spectrum, suggesting that amide groups may be involved in binding to the silver surface and enhancing the stability of AgNPs (Kumar & Mamidyala 2011). Weak symmetrical peaks were observed at 1378 cm^{-1} and 1114 cm^{-1}, and asymmetrical stretching peaks were detected from 1071 to 951 cm^{-1}, indicating the presence of carboxyl groups (Shameli et al. 2012). The biosurfactant spectrum also displayed a peak at 1384 cm^{-1} for carboxyl groups, confirming their role in nanoparticle stabilization by possibly providing negative charges that prevent aggregation (Jain et al. 2011; Tomah et al. 2020). The absorption peak around 668 cm^{-1} corresponds to phosphate groups, which was also present in the biosurfactant spectrum (668 and 602 cm^{-1}) (Rudakiya & Pawar 2017). These spectral assignments are summarized in Table 1.

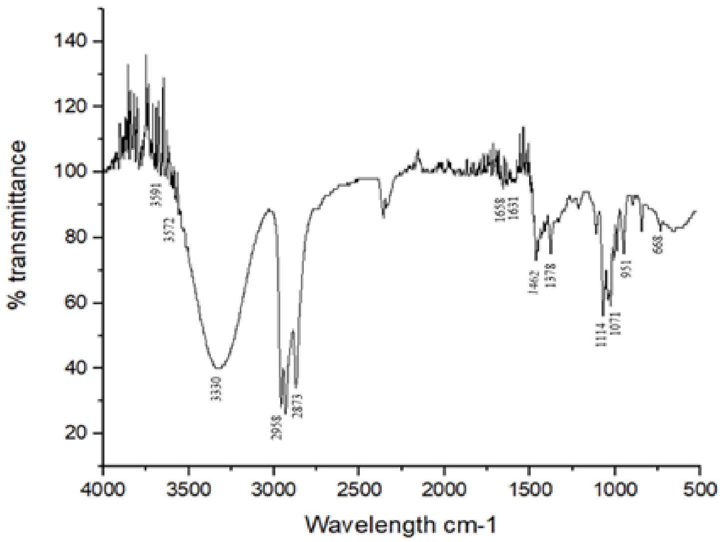

Figure 5. FTIR spectra of biosurfactant-stabilized AgNPs showing the presence of carboxyl (1378 cm^{-1} and 1114 cm^{-1} and 1071 cm^{-1} to 951 cm^{-1}), hydroxyl (3591 cm^{-1}, 3572 cm^{-1}, and 3330 cm^{-1}), alkane (2958 cm^{-1}, 2873 cm^{-1} , and 1462 cm^{-1}), amide (1658 to 1631 cm^{-1}), and phosphate groups 668 cm^{-1}.

The high similarity between the FTIR spectra of the biosurfactant and the biosurfactant-stabilized AgNPs implies that functional groups, including hydroxyl, alkane, amide, carboxyl, and phosphate groups, actively contribute to the stabilization of silver nanoparticles. These functional groups likely act as reducing sites, where hydroxyl (–OH), carboxyl (–COOH), and amino (–NH) groups donate electrons to convert Ag^{+} ions into elemental Ag^{0} (Abd Alamer et al. 2021). During synthesis, the polar functional groups reduce Ag^{+}

Table 1. Fourier-transform infrared spectral characteristics of biosurfactant and AgNPs.

No.	Functional Group	Biosurfactant (cm^{-1})	AgNPs (cm^{-1})	Shift (cm^{-1})	Interpretation
1	O–H stretching (hydroxyl)	3405	3591, 3572, 3330	+186 / +167 / −75	Hydroxyls donate electrons for Ag coordination; broadening indicates stronger interactions
2	C–H stretching (alkane)	2925	2958, 2873	+33 / −52	Aliphatic chains reorganize around Ag surface, contributing to stabilization
3	Amide I (C=O)	1623	1658 –1631	+8 to +35	Protein/peptide carbonyls interact with Ag, shifting carbonyl vibration
4	C–H stretching (alkane)	—	1462	New	Additional aliphatic chains contributing to stabilization
5	Carboxylate (–COO^-)	1384	1378	−6	Carboxylates provide electrostatic stabilization and prevent aggregation
6	Carboxyl/ polysaccharide	—	1114, 1071–951	New	Carbohydrate/carboxylate signals engaged in capping
7	Ester C–O	1105	—	Disappeared	Native ester signal disappears, suggesting participation in Ag binding
8	Phosphate P–O (dual)	668, 602	668	0 / − 66	Phosphate groups act as capping agents; loss of one band indicates binding
9	O–Ag stretching	—	472	New	Direct evidence of Ag–O bond formation

to Ag^0 nuclei, while biosurfactant molecules orient with their hydrophilic polar head toward the silver core and hydrophobic tail outward, forming a protective layer (Javed et al. 2020). This capping layer stabilizes the particles through steric and electrostatic effects, influencing their size and shape. Simultaneously, the polar hydrophilic heads interact with the nanoparticle surface while the hydrophobic chains extend into the medium, providing a capping layer that prevents agglomeration and influences morphology (Javed et al. 2020). This orientation forms a protective barrier that prevents nanoparticle aggregation, provides steric and electrostatic stabilization, and helps control nanoparticle size and morphology (Javed et al. 2020; Abd Alamer et al. 2021; Sidhu et al. 2022). The results indicate that the biosurfactant from *A. pallidus* functions as both a natural bioreductant and a stabilizer, offering a sustainable alternative to synthetic agents in nanoparticle synthesis. This highlights the potential of biosurfactant-mediated nanoparticle synthesis in the development of eco-friendly nanomaterials.

The FTIR findings complement the SEM and EDX analyses, confirming that the biosurfactant plays a critical role in AgNP stabilization. Functional groups such as hydroxyl, carboxyl, and phosphate likely contribute to steric and electrostatic stabilization, consistent with the uniform size and morphology observed in SEM. Taken together, the integration of FTIR and EDX data highlights the pivotal role of *A. pallidus*-derived biosurfactants in enhancing the stability and composition of AgNPs, which strengthens their potential for diverse industrial, biomedical, and environmental applications.

While this study demonstrates the successful stabilization of silver nanoparticles by biosurfactants produced by *A. pallidus*, we acknowledge that their biological or industrial functionalities were not evaluated. Additionally, the study did not include a direct comparison of biosurfactant yield or nanoparticle synthesis efficiency with other thermophilic microorganisms, which would provide stronger benchmarks. Our present work was designed as a proof-of-concept investigation focused on the isolation of *A. pallidus*, biosurfactant-mediated synthesis, and comprehensive physicochemical characterization of AgNPs. Future studies should examine the performance of biosurfactant-stabilized AgNPs in biomedical, agricultural, and industrial contexts and benchmark the activity of *A. pallidus* against established reference strains. Such investigations will be crucial to validate their potential as eco-friendly nanomaterials with real-world applicability.

CONCLUSIONS

This study demonstrates the ability of the thermophilic bacterium *A. pallidus*, isolated from the Badekbek hot spring in the Philippines, to synthesize AgNPs using biosurfactants for stabilization. The biosurfactant-stabilized AgNPs exhibited uniform size distribution and spherical to amorphous shapes, while nonstabilized AgNPs showed irregular morphologies due to agglomeration. The presence of functional groups in the biosurfactant, as indicated by FTIR analysis, played a crucial role in reducing nanoparticle aggregation. Furthermore, EDX analysis confirmed a notable increase in oxygen and carbon content in the biosurfactant-stabilized AgNPs. These findings establish a proof-of-concept that biosurfactants from *A. pallidus* can effectively enhance the stability and quality of AgNPs, providing a sustainable alternative to chemical stabilizers. The potential applications of these stabilized nanoparticles remain to be validated, and future work will assess their antimicrobial, catalytic, and biocompatibility properties, as well as benchmark their performance against reference thermophilic strains.

AUTHOR CONTRIBUTION

M.R., F.C., and M.M. designed the research and collected and analyzed the data. M.R. wrote the manuscript. R.B. supervised all the process.

ACKNOWLEDGMENTS

The authors also thank laboratory personnel of Department of Biology, College of Science, UP Baguio, for lending equipment all throughout the experiment.

CONFLICT OF INTEREST

The authors declare that the research was conducted in the absence of any commercial or financial relationships that could be construed as a potential conflict of interest.

REFERENCES

Abd Alamer, I.S. et al., 2021. Biosynthesis of silver chloride nanoparticles by rhizospheric bacteria and their antibacterial activity against phytopathogenic bacterium *Ralstonia solanacearum*. *Molecules*, 27(1), 224. doi: 10.3390/molecules27010224

Albukhaty, S. et al., 2025. Eco-Friendly Synthesis of Silver Nanoparticles: Principles and Their Antimicrobial Characteristics. In *Sustainable Nanoremediation: Modern Technologies for a Clean Environment*. Apple Academic Press, pp.253-295. doi: 10.1201/9781003468950

Arutchelvi, J. et al., 2009. Production and characterization of biosurfactant from *Bacillus subtilis* YB7. *Journal of Applied Science*, 9(17), pp.3151-3155. doi: 10.3923/jas.2009.3151.3155.

Brock, T.D. & Freeze, H. 1969. Thermus aquaticus gen. n. and sp. n., a non-sporulating extreme thermophile. *Journal of bacteriology*, 98(1), pp.289-297. doi: 10.0000/jb.asm.org/jb/98/1/289.

Busscher, H.J. Neu, T.R. & Van der Mei, H.C., 1994. Biosurfactant production by thermophilic dairy streptococci. *Applied Microbiology and Biotechnology*, 41(1), pp.4-7. doi: 10.1007/BF00166073.

Farias, C.B. et al., 2014. Synthesis of silver nanoparticles using a biosurfactant produced in low-cost medium as stabilizing agent. *Electronic Journal of Biotechnology*, 17(3), pp.122-125. doi: 10.1016/j.ejbt.2014.04.003.

Fayez, A.M. et al., 2011. Biosynthesis of silver and gold nanoparticles using thermophilic bacterium *Geobacillus stearothermophilus. Process Biochemistry*, 46(10), pp.1958-1962. doi: 10.1016/j.procbio.2011.07.003

Gomaa, E.Z., 2016. Exopolysaccharide-mediated silver nanoparticles produced by *Lactobacillus brevis* NM101-1 as antibiotic adjuvant. *Microbiology*, 85, pp.207-219. doi: 10.1134/S0026261716020077

Gonzaga, M.L.C. et al., 2005. Isolation and characterization of polysaccharides from *Agaricus blazei* Murill. *Carbohydrate Polymers*, 60(1), pp.43-49. doi: 10.1016/j.carbpol.2004.11.022.

Hardini, R.D. & Saraswati, T.E., 2023. Concentration dependence of NaBH4 reductant on the optical properties of colloidal silver nanoparticles synthesized from AgNO3 solution. *Journal of Physics: Conference Series*, 2556, 012013. doi: 10.1088/1742-6596/2556/1/012013

Hebeish, A. et al., 2013. Nanostructural features of silver nanoparticles powder synthesized through concurrent formation of the nanosized particles of both starch and silver. *Journal of Nanotechnology*, 2013(1), 201057. doi: 10.1155/2013/201057

Jain, N. et al., 2011. Extracellular biosynthesis and characterization of silver nanoparticles using *Aspergillus flavus* NJP08: a mechanism perspective. *Nanoscale*, 3(2), pp.635-641.

Jara, A.M., Andrade, R.F. & Campos-Takaki, G.M., 2013. Physicochemical characterization of tensio-active produced by *Geobacillus stearothermophilus* isolated from petroleum-contaminated soil. *Colloids and Surfaces B: Biointerfaces*, 101, pp.315-318. doi: 10.1016/j.colsurfb.2012.05.021

Javed, R. et al., 2020. Role of capping agents in the application of nanoparticles in biomedicine and environmental remediation: recent trends and future prospects. *Journal of Nanobiotechnology*, 18, 172. doi: 10.1186/s12951-020-00704-4

Juibari, M. et al., 2011. Intensified biosynthesis of silver and gold nanoparticles using a native extremophilic *Ureibacillus thermosphaericus* strain. *Material Letters*, 65(6) pp.1014-1017. doi: 10.1016/j.matlet.2010.12.056.

Kim, H.S. et al., 1997. Production and properties of a lipopeptide biosurfactant from *Bacillus subtilis* C9. *Journal of fermentation and bioengineering*, 84(1), pp.41-46. doi: 10.1016/S0922-338X(97)82784-5.

Kumar, C.G. & Mamidyala, S.K., 2011. Extracellular synthesis of silver nanoparticles using culture supernatant of *Pseudomonas aeruginosa. Colloids and Surfaces B: Biointerfaces*, 84(2), pp.462-466. doi: 10.1016/j.colsurfb.2011.01.042

Lee, Y.J. et al., 2022. Isolation and characterization of thermophilic bacteria from hot springs in Republic of Korea. *Microorganisms*, 10(12), 2375. doi: 10.3390/microorganisms10122375

Markam, S.S. et al., 2024. Microbial Biosurfactants: Green alternatives and sustainable solution for augmenting pesticide remediation and management of organic waste. *Current Research in Microbial Sciences*, 7, 100266. doi: 10.1016/j.crmicr.2024.100266

Mehetre, G.T., Dastager, S.G. & Dharne, M.S., 2019. Biodegradation of mixed polycyclic aromatic hydrocarbons by pure and mixed cultures of biosurfactant producing thermophilic and thermo-tolerant bacteria. *Science of The Total Environment*, 679, pp.52-60. doi: 10.1016/j.scitotenv.2019.04.376

Nayarisseri, A., Singh, P. & Singh, S.K., 2018. Screening, isolation and characterization of biosurfactant producing *Bacillus subtilis* strain ANSKLAB03. *Bioinformation*, 14(6), 304. doi: 10.6026/97320630014304

Osman, A.I. et al., 2024. Synthesis of green nanoparticles for energy, biomedical, environmental, agricultural, and food applications: A review. *Environmental Chemistry Letters*, 22(2), pp.841-887. doi: 10.1007/s10311-023-01682-3

Płaza, G., Chojniak, J. & Banat, I., 2014. Biosurfactant Mediated Biosynthesis of Selected Metallic Nanoparticles. *International Journal of Molecular Sciences*, 15(8), pp.13720–13737. doi: 10.3390/ijms150813720.

Reddy, A.S. et al., 2009. Synthesis of silver nanoparticles using surfactin: A biosurfactant as stabilizing agent. *Materials letters*, 63(15), pp.1227-1230. doi: 10.1016/j.matlet.2009.02.028.

Rudakiya, D. M. & Pawar, K., 2017. Bactericidal potential of silver nanoparticles synthesized using cell-free extract of *Comamonas acidovorans*: in vitro and in silico approaches. *3 Biotech*, 7(2), 92. doi: 10.1007/s13205-017-0728-3

Saleem, S.S., Saleem, S., & Nazar, M.F., 2023. Role of Biosurfactants in Nanoparticles Synthesis and their Stabilization. *Advancements in Biosurfactants Research*, pp.191-213. doi: 10.1007/978-3-031-21682-4_10

Sarubbo, L.A. et al., 2022. Biosurfactants: Production, properties, applications, trends, and general perspectives. *Biochemical Engineering Journal*, 181, 108377. doi: 10.1016/j.bej.2022.108377

Schultz, J. et al., 2022. Polyphasic Analysis Reveals Potential Petroleum Hydrocarbon Degradation and Biosurfactant Production by Rare Biosphere Thermophilic Bacteria From Deception Island, an Active Antarctic Volcano. *Frontiers in Microbiology*, 13, 885557. doi: 10.3389/fmicb.2022.885557

Shameli, K. et al., 2012. Synthesis and characterization of polyethylene glycol mediated silver nanoparticles by the green method. *International journal of molecular sciences*, 13(6), pp.6639-6650. doi: 10.3390/ijms13066639

Shrestha, S., Wang, B. & Dutta, P., 2020. Nanoparticle processing: Understanding and controlling aggregation. *Advances in colloid and interface science*, 279, 102162. doi: 10.1016/j.cis.2020.102162

Sidhu, A.K., Verma, N. & Kaushal, P., 2022. Role of biogenic capping agents in the synthesis of metallic nanoparticles and evaluation of their therapeutic potential. *Frontiers in Nanotechnology*, 3, 801620. doi: 10.3389/fnano.2021.801620

Singh, P. et al., 2017. Production of biosurfactant stabilized nanoparticles. *International Journal of Pharmaceutical and Biological Sciences*, 8, pp.701-707. doi: 10.22376/ijpbs.2017.8.2.b701-707.

Singla, R.S. et al., 2017. Role of bacteria in nanocompound formation and their application in medical. *Microbial Applications*, 2(1), pp.3-37. doi: 10.1007/978-3-319-52669-0_1.

Tomah, A.A. et al., 2020. Mycosynthesis of silver nanoparticles using screened Trichoderma isolates and their antifungal activity against *Sclerotinia sclerotiorum*. *Nanomaterials*, 10(10), 1955. doi: 10.3390/nano10101955

Vanlalveni, C. et al., 2024. A review of microbes mediated biosynthesis of silver nanoparticles and their enhanced antimicrobial activities. *Heliyon*, 10 (11), e32333. doi: 10.1016/j.heliyon.2024.e32333

Xie, Y., Ye, R. & Liu, H., 2006. Synthesis of silver nanoparticles in reverse micelles stabilized by natural biosurfactant. *Colloids and Surfaces A: Physicochemical and Engineering Aspects*, 2, pp.175–178. doi: 10.1016/j.colsurfa.2005.12.056.

Yateem, A. et al., 2002. Isolation and Characterization of Biosurfactant-Producing Bacteria from Oil-Contaminated Soil. *Soil and Sediment Contamination: An International Journal*, 11(1), pp.41–55. doi: 10.1080/20025891106682.

Yeh, Y., Creran, B. & Rotello, V.M., 2011. Gold nanoparticles: preparation, properties, and applications in bionanotechnology. *Nanoscale*, 4(6), pp.1871-1880. doi: 10.1039/C1NR11188D

Yong P. et al., 2002. Bioaccumulation of palladium by *Desulfovibrio desulfuricans.* J*ournal of Chemical Technology and Biotechnology*, 77(5), pp.593–601. doi: 10.1002/jctb.606.

Zehra, S.H. et al., 2025. Advancements in Green Synthesis of Silver-Based Nanoparticles: Antimicrobial and Antifungal Properties in Various Films. *Nanomaterials*, 15(4), 252. doi: 10.3390/nano15040252

Zheng, C. et al., 2012. Characterization and emulsifying property of a novel bioemulsifier by *Aeribacillus pallidus* YM-1. *Journal of Applied Microbiology*, 113(1), pp.44-51. doi: 10.1111/j.1365-2672.2012.05313.x.